Analysis of a Coaxial, Compact Thermoacoustic Heat-Pump

Gaëlle Poignand, Alexey Podkovskiy, Guillaume Penelet, Pierrick Lotton, Michel Bruneau

Laboratoire d'Acoustique de l'Université du Maine (LAUM), UMR CNRS 6613, Université du Maine, Avenue Olivier Messiaen, 72 085 Le Mans Cedex 9, France. pierrick.lotton@univ-lemans.fr

Summary

An analytical approach to describe the behaviour of a compact thermoacoustic stack-based or regenerator-based heat-pump driven by two acoustic sources has been presented in a previous paper [Acta Acustica united with Acustica **97** (2011) 926–932]. It appears to be suitable for fitting adjustable parameters to achieve optimal heat transfer or temperature gradient, even COP. This model has been used to design such thermoacoustic refrigerators, which involve compactness and flexibility. The predicted characteristics are compared with some experimental results in this paper. Then performance of this small scale thermoacoustic device is compared with the one obtained with standing or travelling wave devices having similar stack/regenerator. Slightly higher efficiency than in the standing wave system is found, whereas the comparison with the coaxial travelling wave configuration gives slightly lower efficiency, yet at much smaller size.

PACS no. 43.35.Ud

1. Introduction

Several attempts to reduce the size of thermoacoustic refrigerators have been carried out since the early 2000's. Initially, some authors proposed to reduce the dimensions of the systems, while maintaining a classical design by raising the acoustic frequency. Thus, miniaturized standing-wave refrigerators were developed using both a piezoelectric actuator as sound source and a micro machined stack whose dimensions are matched with the high working frequency [1, 2, 3]. However, the performance of these systems is limited in terms of heat extracted from the cold source, namely in terms of coefficient of performance (COP).

Then, designs had to be revisited in order to reduce the size of thermoacoustic refrigerators while maintaining their performance. In this context, Tijani *et al.* developed a coaxial travelling-wave (Stirling) cooler [4] based on a structure close to one previously designed by Swift *et al.* [5]. This structure involves a resonator coupled to a lumped element acoustic network which includes the thermoacoustic core (a regenerator with two heat exchangers at its ends), an inertance tube and a compliant cavity. These acoustical inertance and acoustical compliance form a phasing network to produce high acoustic impedance in the regenerator with pressure oscillations and particle velocity in phase, as required by the Stirling cycle. The cooler developed by Tijani *et al.* has the advantage of being more compact because it uses a coaxial topology

for the phasing network instead of the toroidal one used by Swift *et al.* In the same line of thought, Smith *et al.* developed a travelling-wave thermoacoustic refrigerator [6] in which the acoustic resonator and the lumped phasing acoustic network are replaced by a hybrid acoustic-mechanical system. The acoustic resonator being suppressed, it leads to a really compact refrigerator that allows nevertheless achieving rather good performance. However, it does not allow the flexibility of the compact device considered herein (thus preventing it from achieving optimal performance, see below).

More recently, Poignand *et al.* have presented an analytical description of an alternative non-resonant compact thermoacoustic cooler [7]. A sketch of this device is presented in Figure 1. It is composed of a thermoacoustic core (stack or regenerator) set in a small cavity. The thermoacoustic core almost fills the cavity and is surrounded by a peripheral channel. Due to this design, the ends of the stack/regenerator can be considered set on either side of an acoustic inner source (labelled 1) which then creates the monochromatic displacement field needed in the acoustic process, in a frequency range such that the wavelength remains much greater than the dimensions of the cavity. A quasi-uniform pressure field is driven at the same frequency by another source (called outer source, labelled 2) set on a wall of the cavity. In some respect, the structure of this compact device could be considered analogous to the one developed by Smith *et al.*, but providing more flexibility because the working frequency, the amplitude and the phase difference between the pressure and the velocity fields can be tuned for optimizing the performance of the device. Indeed, the acoustic pressure and the par-

ticle velocity are not linked anymore by standing wave or travelling wave conditions, and can then be managed independently when tuning both the outer source and the inner source.

In 2006, Poignand *et al.* [8] have shown analytically that the thermoacoustic process in a stack can be optimized when tuning the acoustic field to optimal values of the acoustic pressure amplitude, the particle velocity amplitude, and their relative phase. According to linear theory, the temperature gradient along the stack is proportional to the amplitude of the acoustic pressure. So, an acoustic pressure level as high as possible is obviously required to maximise the thermoacoustic process. Beside, optimal value for the amplitude of the particle velocity $|u|_{opt}$ (which is different from its maximal value) and optimal value of the relative phase φ_{opt} can be found after deriving the analytical expression of the temperature gradient, independently with respect to variables $|u|$ and φ. Optimal values are reached when the derivative is zero. These optimal values depend on the frequency, on the shape and the dimensions of the stack/regenerator, and on the thermophysical properties of the fluid and the stack/regenerator [7]. Alternatively, these optimal values can be obtained by numerical simulation, for example using DeltaEC (which is a specific numeric code to design thermoacoustic devices [9]).

This optimal field can easily be tuned within the stack/regenerator of the non resonant compact thermoacoustic device considered herein. The analytical model developed in [7] allows the prediction of the theoretical temperature difference and COP obtained in such a device tuned at its optimal operating point. This theoretical performance has then been compared with that of a conventional half-wavelength acoustic refrigerator, using similar quasi-adiabatic stacks in both devices. This comparison leads us to conclude that, in addition to its interesting compactness, the device considered herein could provide higher performance in terms of COP or temperature difference between the two ends of the stack.

The main purpose of the present paper is twofold. Firstly, the existence of an optimal acoustic field for the thermoacoustic process is investigated experimentally (namely from measurements on the compact thermoacoustic refrigerator using either quasi-adiabatic stack or quasi-isothermal regenerator). It is established that this optimal field corresponds to that predicted by the theoretical model. Secondly, being concerned by the global efficiency, the performance of the non-resonant compact thermoacoustic refrigerator is evaluated theoretically in terms of temperature difference ΔT, thermoacoustic heat flux Q, and global efficiency η (defined as the ratio between the thermoacoustic heat flux Q and the electric power P_{el} provided to the loudspeakers). This performance is then compared with those of classical devices having equivalent stack/regenerator (standing wave device and travelling wave coaxial device) available in the literature, showing the potentiality of this compact thermoacoustic cooler and its interest from a practical point of view.

Table I. Dimensions of the compact thermoacoutic device under test.

Length of the cylindrical cavity	L	10.2 cm
Internal diameter of the cavity	d	9.4 cm
Length of the stack	l_{st}	4 cm
Diameter of the stack	d_{st}	8 cm
Thickness of the peripheral channel	e_{ch}	0.7 cm

2. Experimental determination of the optimal acoustic field

2.1. Experimental set up

A view of the compact thermoacoustic cooler under test is shown in Figure 1 and its dimensions are given in Table I. The thermoacoustic core is set in a cylindrical small cavity and surrounded by a peripheral channel. The gas filling the cavity is air at atmospheric pressure and room temperature. The acoustic field in the thermoacoustic core is controlled by two electrodynamic loudspeakers. The loudspeaker 2 (PHL audio 1590), set at one extremity of the cavity, creates the acoustic pressure field in the stack, while the velocity is essentially controlled by the loudspeaker 1 (Visaton SC 8N) set inside the cavity. In practice, both loudspeakers 1 and 2 have to be correctly tuned in amplitude and in phase in order to generate the required velocity in the stack.

The experiments are conducted with either a quasi-adiabatic stack or a quasi-isothermal regenerator without any heat exchangers. The quasi-adiabatic stack consists of a ceramic porous material with 600 cells per square inch and a porosity of 80%. Each channel has a cross-section of $600 \times 600\,\mu m^2$. The quasi-isothermal regenerator is composed of stainless steel meshes with a hydraulic radius $r_h = 183\,\mu m$ and exhibits a porosity of 85%. The working frequencies are chosen in such a way that the ratio between the hydraulic radius r_h and the thermal boundary layer δ_h is around 3 for the stack (i.e. $f = 200\,Hz$) and around 0.5 for the regenerator (i.e. $f = 50\,Hz$). These working frequencies are such that the wavelength is much larger than the dimensions of the compact thermoacoustic cavity.

The instrumentation of the device is schematically presented in Figure 1a. A microphone (Brüel & Kjær type 4938) flush mounted on the wall of the cylindrical cavity measures the acoustic pressure p_{mic} in this cavity. The microphone sensitivity is 1.43 mV/Pa with a specified accuracy of 0.05 mV/Pa. The oscillating velocity u_{memb} of the membrane of the loudspeaker 1 is also measured by means of a laser vibrometer (Polytec OFV 3001). This is realized by drilling a hole through the magnetic motor of the loudspeaker, so that the laser beam is reflected by the rear side of the moving membrane. The amplitude error specified by the vibrometer manufacturer is 3.5% of the velocity amplitude. So, the amplitude p of the acoustic pressure averaged over the length of the stack/regenerator, the amplitude u of the acoustic velocity averaged over both the section and the length of the stack/regenerator and the phase difference $\varphi = \varphi_u - \varphi_p$ between both pressure and velocity can be
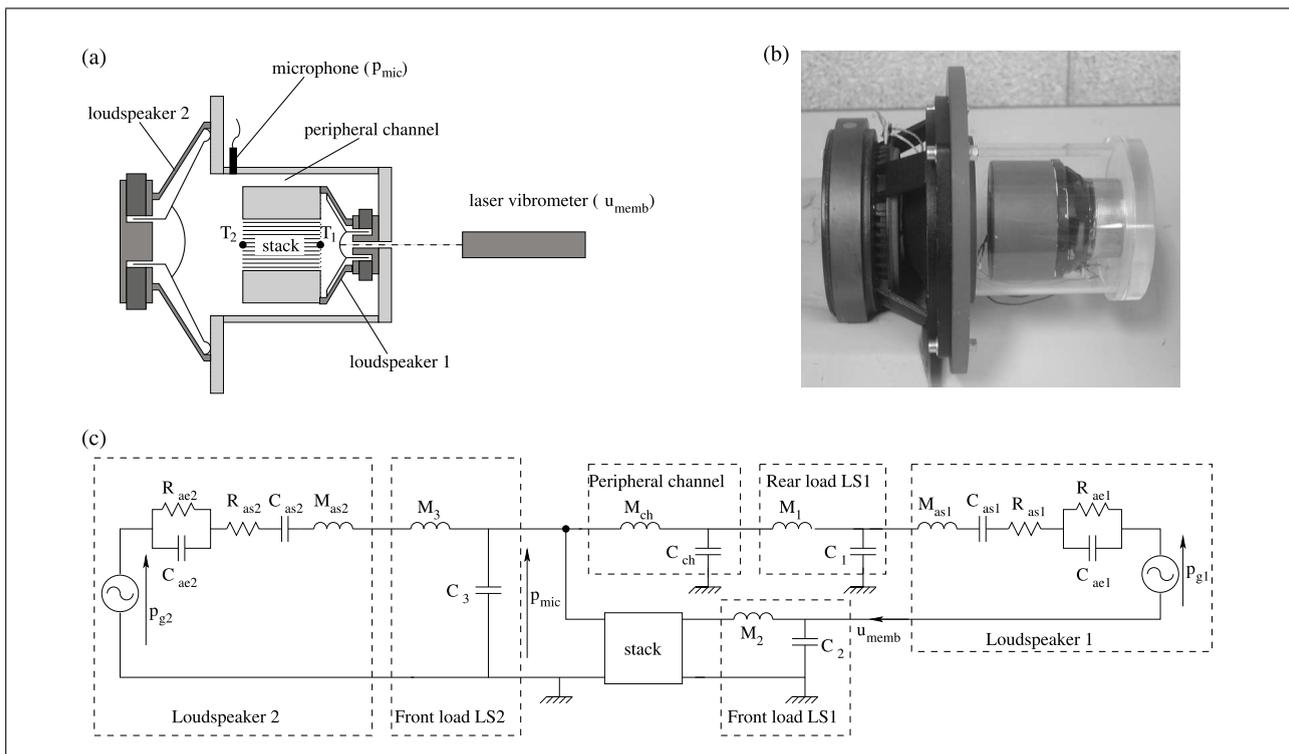
Figure 1. Schematic view (a) and photograph (b) of the device under test. Electrical network equivalent to the device under test (c) where p_{gi}, R_{aei}, C_{aei}, R_{asi}, C_{asi}, and M_{asi}, are the acoustical representations of the voltage provided to loudspeaker "i", the resistance of the voice coil, the inductance of the voice coil, the mechanical resistance, the mechanical compliance and the mass of the moving part of the loudspeaker "i", respectively [16], and where the acoustical compliance and the acoustical mass of each volume of the device are represented by a capacitance C and an inertance M, respectively.

deduced from the acoustic pressure p_{mic} and the membrane velocity u_{memb}, by means of the lumped-element electroacoustic model given in Figure 1c [7] or equivalently by modelling the device with DeltaEC. The uncertainty on the phase φ is estimated to be less than 3°. The temperature difference $\Delta T = T_2 - T_1$ between the stack ends is measured by means of a digital two channels T-type thermocouples thermometer (RS 1314) with an accuracy of $\pm 0.3\,°\mathrm{K}$.

Experimental results, namely herein the temperature difference between the stack ends, showing the influence of the three acoustic parameters (the acoustic pressure amplitude p, the particle velocity amplitude u and the relative phase $\varphi = \varphi_u - \varphi_p$) on the compact system performance are presented below for both a stack and a regenerator. The effect of each of the three acoustic parameters is investigated independently by fixing the two others parameters at their theoretical optimal value. The uncertainties associated with each measured value are presented with error bars.

2.2. Results for a stack-based thermoacoustic cavity

For the quasi-adiabatic stack described in the previous section, the analytical [8] optimal values of the acoustic pressure amplitude p, the particle velocity amplitude u_{opt} and the phase φ_{opt} are given in Table II. Note that in this setup, the pressure peak amplitude is set to $p = 1000\,\mathrm{Pa}$ which

Table II. Theoretical values of the optimal acoustic field in the stack/regenerator and theoretical temperature differences.

Quasi-adiabatic stack	Quasi-isothermal stack
$p = 1000\,\mathrm{Pa}$	$p = 1000\,\mathrm{Pa}$
$u_{opt} = 1.43\,\mathrm{m/s}$	$u_{opt} = 1.26\,\mathrm{m/s}$
$\varphi_{opt} = 3\pi/4\,\mathrm{rad}$	$\varphi_{opt} = 2.9\,\mathrm{rad}$
$\Delta T_{max,th} = 15.8\,\mathrm{K}$	$\Delta T_{max,th} = 16.6\,\mathrm{K}$

is close to the maximum pressure that can be generated by the loudspeaker 2 without harmonic distorsion.

Figure 2a shows the evolution of the temperature difference ΔT normalized by its maximum value ΔT_{max} as a function of the acoustic pressure p when $u = u_{opt}$ and $\varphi = \varphi_{opt}$. As predicted by the linear steady state theory [10] (solid line), the experimental results obtained (crosses) show that the temperature difference ΔT increases with acoustic pressure. However, for the maximum acoustic pressure of $1000\,\mathrm{Pa}$, the temperature difference at the stack ends reaches $\Delta T_{max,exp} = 10.3\,\mathrm{K}$, which is smaller than the theoretical one $\Delta T_{max,th} = 15.8\,\mathrm{K}$. This discrepancy mainly arises from the neglect of numerous, complicated heat transfer processes at the ends of the stack [11].

Figure 2b shows the evolution of the temperature difference ΔT normalized by its maximum value ΔT_{max} as a function of the velocity amplitude u (when $p = p_{max}$
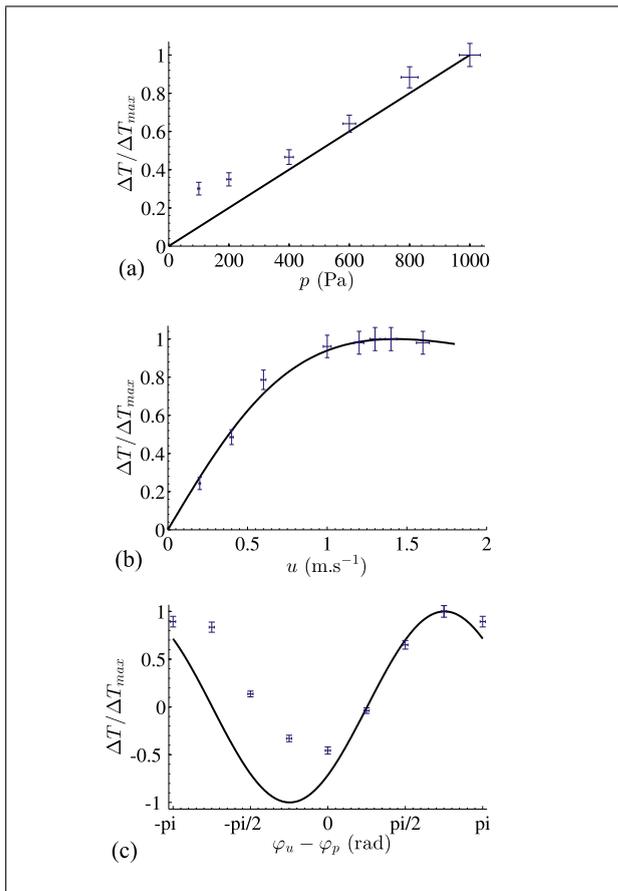
Figure 2. Normalized temperature difference $\Delta T/\Delta T_{max}$ between the stack ends measured (×) and calculated (straight line) as a function of (a) the acoustic pressure p, (b) the particle velocity amplitude u and (c) the phase φ between the particle velocity and the acoustic pressure.

Figure 3. Temperature difference ΔT between the regenerator ends measured (×) and calculated (straight line) as a function of (a) the acoustic pressure p, (b) the particle velocity amplitude u and (c) the phase φ between the particle velocity and the acoustic pressure.

and $\varphi = \varphi_{opt}$). A good agreement is obtained between the theoretical predictions (solid line) and the experimental results (crosses). Especially, the experimental optimal velocity amplitude is found close to the theoretical one ($u_{opt} = 1.4\,\text{m/s}$).

The normalized temperature difference $\Delta T/\Delta T_{max}$ versus the relative phase φ (when $p = p_{max}$ and $u = u_{opt}$) is shown in Figure 2c. When the phase shift φ varies between $(-3\pi/4)$ and $(\pi/4)$, the temperature difference $\Delta T/\Delta T_{max}$ is positive and the cold-side of the stack is near the loudspeaker 1 controlling the velocity, whereas for a phase φ comprised between $\pi/4$ and $5\pi/4$, the temperature difference is negative and the cold-side stack end is located near the loudspeaker 2 controlling the pressure. Thus, it is worth noting that the cold-side stack end location can be fixed by the phase φ. From the experimental results presented in Figure 2c, it can be noticed that there is an optimal phase $\varphi_{opt,exp} = 3\pi/4$ rad which corresponds to the theoretical optimal phase. However, the evolution of the experimental normalized temperature difference does not fit completely the theoretical one. This difference is due to the heating of the loudspeaker voice-coil controlling the velocity. This h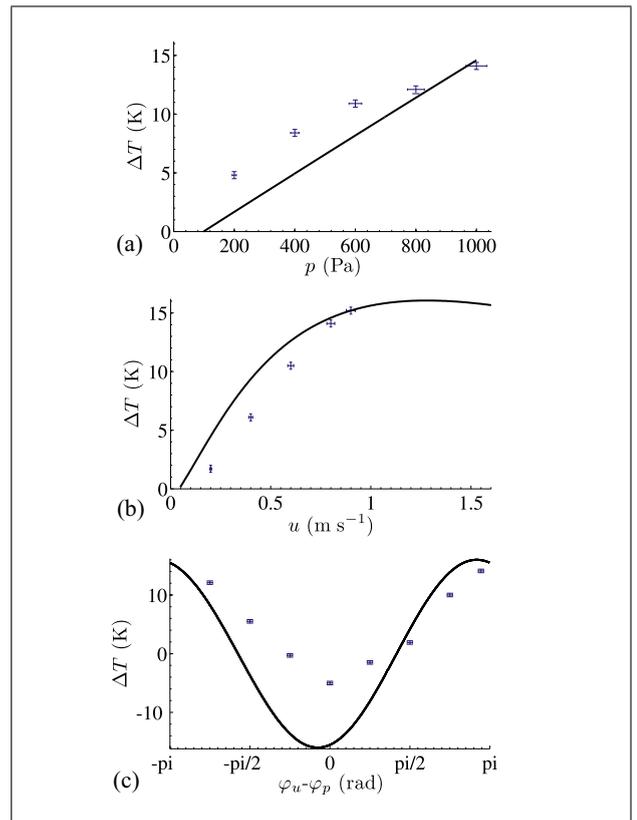eating is added to the thermoacoustic heat flux and leads to an increase of the stack end temperature near the loudspeaker 1.

2.3. Results for a regenerator-based thermoacoustic cavity

For the isothermal regenerator described in section 1.1, the theoretical optimal values of the acoustic pressure amplitude p, the particle velocity amplitude u_{opt} and the phase φ_{opt} are given in Table II. These values are determined numerically from the software DeltaEC, when setting the pressure amplitude to its maximal value (1000 Pa) and tuning the values of velocity amplitude and phase to those which lead to a maximum temperature difference.

Figure 3a shows the temperature difference ΔT versus the acoustic pressure when $\varphi = \varphi_{opt}$ and when the amplitude of the particle velocity is set to $u = 0.8\,\text{m/s}$. This velocity amplitude corresponds to the maximum amplitude which can be reached with loudspeaker 1 in this regenerator-based device. Consequently, the amplitude of the particle velocity is not set to its optimal value $u_{opt} = 1.26\,\text{m/s}$. However, the conclusions remain valid because the optimal phase and the optimal acoustic pressure are independent of the value of the particle velocity u. As expected, both the measured and predicted temperature differences increase with the acoustic pressure. Note that the

theoretical values of ΔT_{th} are calculated by adjusting the regenerator thermal conductivity in order to fit the experimental temperature difference value $\Delta T_{exp} = 14.1$ K measured when $p = 1000$ Pa. Actually, the effective thermal conductivity of the regenerator is lower than the thermal conductivity of the regenerator material due to the poor contact between adjacent screens in the regenerator. This is usually taken into account in theoretical approaches by an empirical degradation factor between 0.1 and 0.2 [12, 13, 14]. In our case, this factor is set to 0.19.

Figure 3b represents the temperature difference ΔT as a function of the velocity amplitude u (when $p = p_{max}$ and $\varphi = \varphi_{opt}$). The theoretical curve (solid line) exhibits the same trend as the experimental one (crosses), even if the optimal value of the particle velocity $u_{opt} = 1.26$ m/s cannot be reached. The experimental determination of the optimal velocity amplitude would require to change the loudspeaker 1 or to design a new setup with appropriate geometrical characteristics.

Finally, Figure 3c represents the influence of the relative phase φ on the temperature difference when $u = 0.8$ m/s and $p = p_{max}$. The presence of an experimental optimal value for the relative phase φ is highlighted. This value roughly corresponds to the theoretical one $\varphi_{opt} = 2.9$ rad.

3. Performances of the compact cooler, discussions

In this section, the behaviour of the small cavity cooler described in the previous section is theoretically compared with the behaviour of both a standing wave cooler and a travelling wave thermoacoustic refrigerator with a coaxial configuration.

3.1. Comparison with a standing wave cooler

A sketch of the standing wave cooler considered for the comparison is presented in Figure 4a. It consists of a half wavelength straight resonator driven by an acoustic source. The fluid filling the resonator is air at atmospheric pressure and room temperature. The source is chosen to be the same electrodynamic loudspeaker as the one which controls the acoustic pressure field in the small cavity cooler described in section 1.1. The resonator length $L_s = 0.65$ m is adjusted in such a way that the resonance frequency of the system is the working frequency of the compact device, i.e. $f = 200$ Hz. The same stack is used for both the compact device and the standing wave cooler. In the standing wave cooler, the stack is set at its better location along the resonator for which the temperature difference is maximal [8], i.e. 0.55 m away from the loudspeaker in our case. The small cavity cooler is set at its optimal working point (given in Table III). To fulfill the comparison of the two devices, their achieved temperature difference ΔT, thermoacoustic heat flux Q and global efficiency η, are compared when the same electric power is provided to the sources (here, $P_{el} = 7.7$ W). Actually, in the case of the compact device, P_{el} represents the total electric power provided to the two loudspeakers. Both
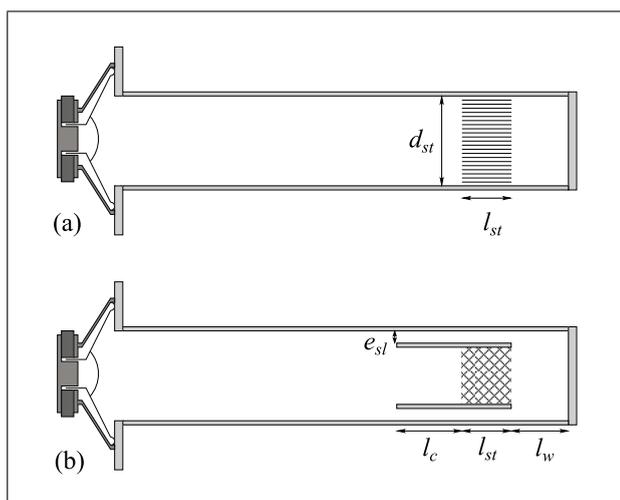

Figure 4. Schematic view of a standing wave cooler (a) and of a travelling wave coaxial cooler (b).

Table III. Theoretical comparison between the behaviour of a small cavity cooler and the behaviour of a standing wave cooler.

Small cavity cooler	Standing wave cooler
Acoustic field in the stack	
$p = 1000$ Pa	$p = 1335$ Pa
$u_{opt} = 1.43$ m/s	$u_s = 1.27$ m/s
$\varphi_{opt} = 3\pi/4$ rad	$\varphi_s = \pi/2$ rad
Theoretical performance	
$\Delta T_{max} = 15.8$ K	$\Delta T_s = 13.8$ K
$Q_{max} = 0.17$ W	$Q_s = 0.15$ W
$P_{el} = 7.7$ W	$P_{el,s} = 7.7$ W
$\eta = 2.14\%$	$\eta = 1.88\%$

the theoretical acoustic field in the stack and the theoretical performance estimated with the software Delta EC are given in Table III for both systems.

The temperature difference reached in the compact system is greater than the one reached in the standing wave cooler. As already mentioned [8], it results from the fact that the operating point in a resonant system imposes a compromise between acoustic pressure and particle velocity in the stack. Hence, even if the acoustic pressure is higher in the resonant system, the velocity amplitude and the relative phase are not the optimal ones for the temperature difference.

The global efficiency η is higher for the small cavity despite the use of two sources. Therefore, the stack-based small cavity cooler has both advantages of being compact and being more efficient than a classical standing wave thermoacoustic cooler. Furthermore, the compact device is easily tunable in terms of operating frequency, and even concerning the direction of the acoustically induced temperature gradient.

Table IV. Theoretical comparison between the behaviour of a small cavity cooler and the behaviour of a coaxial travelling wave cooler.

Small cavity cooler	Coaxial cooler
Acoustic field in the stack	
$p = 1000\,\text{Pa}$	$p = 1166\,\text{Pa}$
$u_{\text{opt}} = 1.26\,\text{m/s}$	$u_t = 1.26\,\text{m/s}$
$\varphi_{\text{opt}} = 2.9\,\text{rad}$	$\varphi_t = 2.9\,\text{rad}$
Performances	
$\Delta T_{\text{max}} = 16.6\,\text{K}$	$\Delta T_t = 18.6\,\text{K}$
$Q = 0.15\,\text{W}$	$Q_t = 0.17\,\text{W}$
$P_{\text{el}} = 0.96\,\text{W}$	$P_{\text{el},t} = 0.96\,\text{W}$
$\eta = 15.6\%$	$\eta_t = 17.7\%$

3.2. Comparison with a travelling wave cooler

The travelling wave thermoacoustic refrigerator considered for the comparison is the coaxial device schematized in Figure 4b. This refrigerator is composed of a linear motor (Q-drive 1S175D) coupled to a resonator in which a regenerator unit (namely the regenerator itself extended by an additional straight duct of length l_c) is placed at a distance l_w from the closed end of the resonator. The fluid filling the resonator is air at atmospheric pressure and room temperature. The regenerator unit section is smaller than the resonator section. Then, a peripheral slit of width e_{sl} forms an acoustic feedback path around the regenerator unit. This geometry allows tuning the acoustic field in the regenerator to its optimal working point by varying the three parameters l_c, l_w and e_{sl} [4]. For this study, the three parameters are tuned to $l_c = 0.6\,\text{cm}$, $l_w = 63\,\text{cm}$ and $e_{sl} = 1\,\text{cm}$. The resonator length $L_s = 3.39\,\text{m}$ is adjusted in such a way that the resonance frequency of the system is the working frequency of the compact device, i.e. $f = 50\,\text{Hz}$. The same regenerator is used for both the compact device and the travelling wave cooler. The source which controls the acoustic pressure field in the small cavity cooler is chosen here to be the same linear motor as the one coupled to the travelling wave resonator.

Both the theoretical acoustic field in the regenerator and the theoretical performance estimated with the software Delta EC are given in Table IV for both the compact and the coaxial devices. Here again, the same electric power is provided to the sources (here $P_{\text{el}} = 0.96\,\text{W}$). As expected, the theoretical temperature differences, thermoacoustic powers and global efficiencies obtained with both regenerator-based devices are much greater than the ones obtained with stack-based devices, since standing wave devices cannot achieve as high a thermodynamic performance as travelling wave devices [15].

When comparing the theoretical behaviour of both regenerator-based devices, it is clear that the coaxial device leads to better results. Global efficiency, for example, is around 13.5% greater for the coaxial device. It is due to the fact that the acoustic pressure is higher in the resonant system for a given input electric power, while velocity amplitude and the relative phase can be tuned to their optimal values in both devices. Nevertheless, performance reached with small cavity cooler remains interesting when compactness is needed (10 cm long cavity against 3.39 m long resonator, in our study). In addition, it is worth noting that the operation of the compact system is much more flexible since the optimal working point can be easily monitored in real time while the design of the coaxial system imposes a fixed operating point.

4. Conclusion

The experimental results presented here illustrate the thermal behaviour of both stack-based and regenerator-based compact thermoacoustic devices as a function of the acoustic field inside the stack/regenerator. They validate theoretical results given in a previous paper [7], namely the existence of an optimal acoustic field leading to better performance in terms of temperature difference, heat flux or COP. Then, a theoretical comparison with performance reached with classical devices having equivalent stack/regenerator (standing wave device or travelling wave coaxial device) show the potentiality of this compact thermoacoustic cooler. In particular, slightly higher efficiency than in the standing wave system is found, whereas the comparison with the coaxial travelling wave configuration gives slightly lower efficiency, yet at much smaller size.

References

[1] T. J. Hofler, J. A. Adeff: A miniature thermoacoustic refrigerator for integrated circuits. 17th International Congress on Acoustics, Rome, September 2-7 2001, 119.

[2] B. Lihoreau, P. Lotton, M. Bruneau, V. Gusev: Piezoelectric source exciting thermoacoustic resonator: Analytical modelling and experiment. Acta Acustica united with Acustica **88** (2002) 986–997.

[3] O. G. Symko, E. Abdel-Rahman, Y. S. Kwon, M. Emmi, R. Behunin: Design and development of high-frequency thermoacoustic engines for thermal management in microelectronics. Microelectronics Journal **35** (2004) 185–191.

[4] M. E. H. Tijani, S. Poelstra: Study of a coaxial thermoacoustic Stirling cooler. Cryogenics **48** (2008) 77–82.

[5] G. Swift, S. Backhaus, D. Gardner: Travelling-wave device with mass flux suppression. US Patent no. 6032464, March 2000.

[6] R. Smith, M. Poese, S. Garrett, R. Wakeland: Thermoacoustic device. US Patent no. 0192324 A1, Oct. 2003.

[7] G. Poignand, P. Lotton, G. Penelet, M. Bruneau: Thermoacoustic, small cavity excitation to achieve optimal performance. Acta Acustica united with Acustica **97** (2011) 926–932.

[8] G. Poignand, B. Lihoreau, P. Lotton, E. Gaviot, M. Bruneau, V. Gusev: Optimal acoustic field in compact thermoacoustic refrigerators. Appl. Acoust. **68** (2007) 642–659.

[9] W. Ward, G. W. Swift: Design environment for low amplitude thermoacoustic engine. J. Acoust. Soc. Am. **95** (1994) 3671–3672.

[10] G. W. Swift: Thermoacoustic engines. J. Acoust. Soc. Am. **84** (1988) 1145–1180.

[11] P. Lotton, P. Blanc-Benon, M. Bruneau, V. Gusev, S. Duffourd, M. Mironov, G. Poignand: Transient temperature

profile inside thermoacoustic refrigerators. Int. J. Heat Mass Trans. **52** (2009) 4986–4996.

[12] M. A. Lewis, T. Kuriyama, F. Kuriyama, R. Radebaugh: Measurement of heat conduction through stacked screens. Adv. in Cryogenic Engineering **43B** (1998) 1611–1618.

[13] G. W. Swift: A unifying perspective for some engines and refrigerators. Acoustical Society of America, Melville, 2002.

[14] M. Telesz: Design and testing of a thermoacoustic power converter. MS thesis, Georgia Institute of Technology, 2006.

[15] P. H. Ceperley: A pistonless stirling engine-the traveling wave heat engine. J. Acoust. Soc. Am. **66** (1979) 1508–1513.

[16] M. Rossi: Acoustics and electroacoustics. Artech House, Incorporated, 1988.